Available online at www.sciencedirect.com
SCIENCE DIRECT®
Applied Radiation and Isotopes 62 (2005) 73–81
Applied Radiation and Isotopes
www.elsevier.com/locate/apradiso

Activation cross-sections of long-lived products of proton-induced nuclear reactions on zinc

F. Tárkányi[a,*], F. Ditrói[a], J. Csikai[a,b], S. Takács[a], M.S. Uddin[c], M. Hagiwara[c], M. Baba[c], Yu.N. Shubin[d], A.I. Dityuk[d]

[a]*Institute of Nuclear Research of the Hungarian Academy of Sciences, POB 51, Debrecen H-4001, Hungary*
[b]*Institute of Experimental Physics, Debrecen University, 4010 Debrecen-10, Pf. 105, Hungary*
[c]*Cyclotron and Radioisotope Center, Tohoku University, Sendai, Japan*
[d]*Institute of Physics and Power Engineering, Obninsk, Russian Federation*

Received 23 February 2004; received in revised form 1 June 2004; accepted 11 June 2004

Abstract

In the frame of a systematic study of excitation functions induced by medium energy protons, the activation cross-sections on natural zinc were investigated for different applications. Excitation functions for production of ^{66,67}Ga, ^{62,65,69m}Zn, ^{64}Cu, ^{57}Ni, ^{55,56,57,58}Co and ^{52,54}Mn radioisotopes were measured by the stacked foil technique in the energy range of 26–67 MeV. Results were compared with the earlier reported experimental data and theoretical calculations based on the ALICE-IPPE code. Experimental data are presented for the first time for most of the products in the investigated energy range. Applications of the measured data for validating the cross-sections on highly enriched isotopic Zn targets and for thin layer activation method are discussed.

Keywords: Zinc; Activation cross-section; Proton induced reactions; Zn, Ga, Cu, Ni, Co and Mn Isotopes

1. Introduction

Intermediate energy activation data are required in different applications: medical radioisotope production, spallation neutron sources, radiation and shielding effects in space, accelerator technology, and radiation therapy. Intermediate energy generally covers a very large energy interval, e.g. from 20 MeV up to several GeV. It has to be mentioned that the different applications are overlapping; therefore, the experimental data usually can be used in various fields. The importance of different nuclear data is very different. Out of them the activation cross-sections on different structural and instrumentation materials induced by proton reactions have primary importance. A survey of the literature shows that the medium energy data are scanty and discrepant. Nowadays only very few groups are engaged with systematic investigations by using modern experimental techniques and methods. However, the accurate theoretical predictions of reaction cross-sections are directly based on precise experimental data or as the result of a well-tested model calculations.

The Debrecen Group has made a systematic study on charged particle activation cross-sections with many elements mostly to set recommended data base for medical applications, thin layer activation technique and

*Corresponding author. Tel.: 36-52-417266; fax: 36-52-416181.
E-mail address: tarkanyi@atomki.hu (F. Tárkányi).

0969-8043/$ - see front matter © 2004 Elsevier Ltd. All rights reserved.
doi:10.1016/j.apradiso.2004.06.008

for monitoring the charged particle beam parameters. For energies below 30 MeV, several detailed experimental data sets exist both on natural and enriched Zn targets. Data is available mostly for the production of medically important ^{66}Ga, ^{67}Ga, ^{64}Cu and for ^{65}Zn. Above 40 MeV for production of medically related ^{62}Zn(^{62}Cu) generator system, only the cross-sections of ^{62}Zn were investigated in detail using natural Zn target. Thanks to the collaboration between the Cyclotron and Radioisotope Centre (CYRIC), Tohoku University, Sendai and the Debrecen Group, the investigations could be extended for higher beam energies. The measurements were made in the frame of a systematic study on the activation cross-sections of light ion-induced nuclear reactions up to 100 MeV. In this paper the experimental activation cross-sections on Zn in the energy range of 26–67 MeV for 13 different products are presented.

2. Experimental

The irradiation technique, the activity determination and the data evaluation were similar to those described in detail previously (Szelecsényi et al., 1998; Ido et al., 2002). In this paper the most salient features of the used experimental technique are presented. The excitation functions were measured by using the stacked foil irradiation technique. One stack was prepared by inserting Zn target foils (650 μm thick), Cu (50 μm thick) and Al (100 μm thick) monitor foils together in sequence. The used stack covered the 67–27 MeV activation energy range. The applied large number of Al and Cu monitor foils allowed to determine simultaneously the excitation functions of the ^{nat}Al(p,x)^{22,24}Na and ^{nat}Cu(p,x)^{56,58}Co,^{62,65}Zn reactions in the given energy interval taking into account the energy degradation and the intensity of the bombarding beam in the stack. The secondary effects of the background neutrons on the Zn target were checked by foils placed in the stack far behind the range of the fully stopped proton beam. The irradiation was done with 70 MeV protons at the external beam of the Tohoku University cyclotron. The activity was measured non-destructively using HPGe detector-based gamma spectrometers. The primary input parameters used for the cross-section calculations were taken from the following publications or determined in the following way. The beam parameters were deduced from monitor reactions (Tárkányi et al., 2001; Ido et al., 2002); the number of the target nuclei was determined via precise weighing of the samples having well-defined surfaces; the number of radioactive nuclei was determined from the activity measured for each of the investigated isotope; the decay parameters collected in the Table 1 were used (Chu et al., 1999); the energy in the middle of the target foils was determined by calculation of the energy degradation (Andersen and Ziegler, 1977); the calculated energy scale was cross-checked with that determined by using the monitor reactions applying a method based on the "flux constancy" (Tárkányi et al., 1991). Direct and cumulative production cross-sections discussed separately for all products were calculated, considering Zn a mono-isotopic element.

The uncertainty of the measured cross-sections was estimated by summing in quadrature of the uncertainties originated from the foil thickness (1%), the incident proton flux (7%), the calculated detector efficiency (5%) and the count rate determination of the photo peak areas of the gamma-lines (1–10%). The change of the beam intensity along the foil stacks was neglected. Uncertainties of the parameters like irradiation time, cooling time, measuring time and half lives contributing nonlinearly to the cross-section formula were not taken

Table 1
Decay data of the investigated reaction products

Nuclide	Half-life	E_γ (keV)	I_γ (%)	Nuclide	Half-life	E_γ (keV)	I_γ (%)
^{66}Ga	9.49 h	1039.2	36.9	^{55}Co	17.53 h	477.2	20.2
						931.2	75.0
^{67}Ga	3.2612 d	184.6	21.2	^{56}Co	77.7 d	846.8	99.9
		300.2	16.8			1238.3	67.0
^{62}Zn	9.186 h	548.4	15.3	^{57}Co	271.77 d	122.1	85.4
		596.6	26.0			136.5	10.69
^{65}Zn	244.06 d	1115.5	50.60	^{58g}Co	70.916 d	810.9	99.5
^{69m}Zn	13.76 h	438.6	94.77	^{60}Co	5.271 yr	1173.2	99.9
						1332.5	99.9824
^{64}Cu	12.7 h	1345.8	0.473	^{52}Mn	5.591 d	744.2	90.0
						935.5	94.5
						1434.1	100
^{57}Ni	35.6 h	1377.6	81.7	^{54}Mn	312.2 d	834.8	99.95

Isotopic abundances of natural Zinc (%):^{64}Zn-48.6, ^{66}Zn-27.9, ^{67}Zn-4.1, ^{68}Zn-18.8, ^{70}Zn-0.6.

into account (Guide to Expression of Uncertainty in Measurement, 1993). The resulted average uncertainty was found to be around 12%. The average uncertainty of the bombarding proton energy in the middle of the target foils estimated from the uncertainties in the primary energy of the beam and the foil thickness was between 0.3 and 2.0 MeV.

3. Results and discussion

Figs. 1–13 show the present experimental results together with the previous measurements. The new numerical data are summarized in Tables 2 and 3. Theoretical calculations done for each product up to 100 MeV proton energy by using the simple but successful ALICE-IPPE model code (Dityuk et al., 1998) rendered to understand the weight of the different

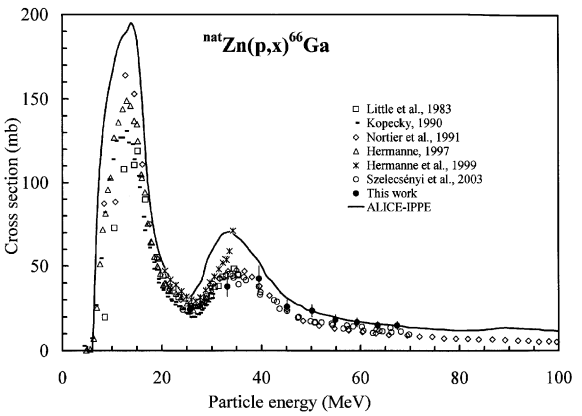

Fig. 1. Experimental and theoretical excitation function for production of ^{66}Ga by proton irradiation of Zn.

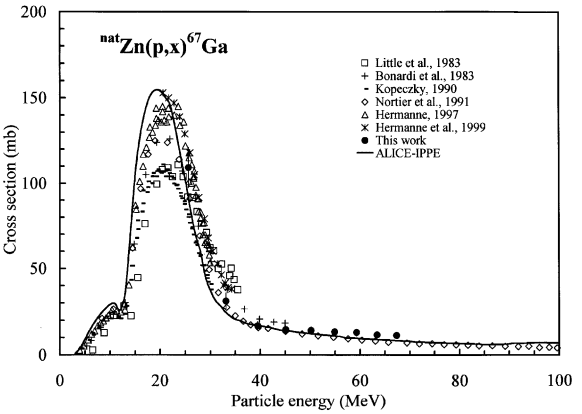

Fig. 2. Experimental and theoretical excitation function for production of ^{67}Ga by proton irradiation of Zn.

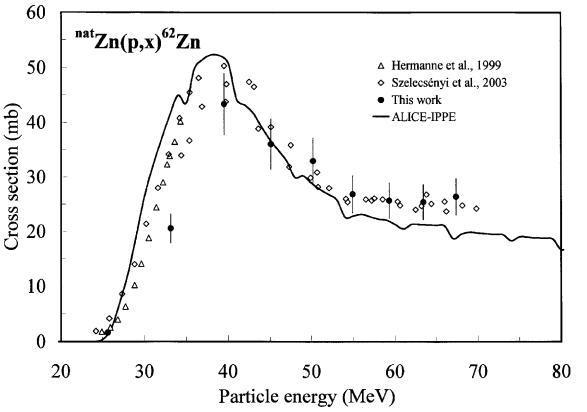

Fig. 3. Experimental and theoretical excitation function for production of ^{62}Zn by proton irradiation of Zn.

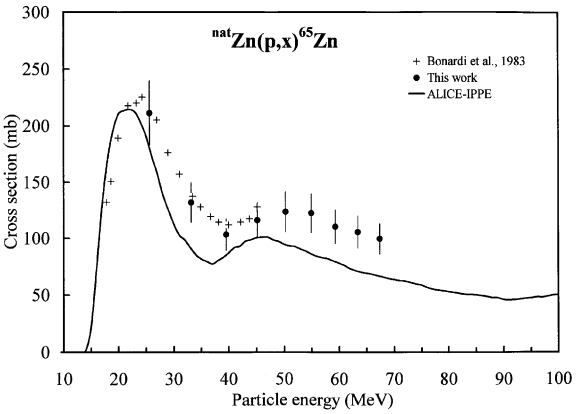

Fig. 4. Experimental and theoretical excitation function for production of ^{65}Zn by proton irradiation of Zn.

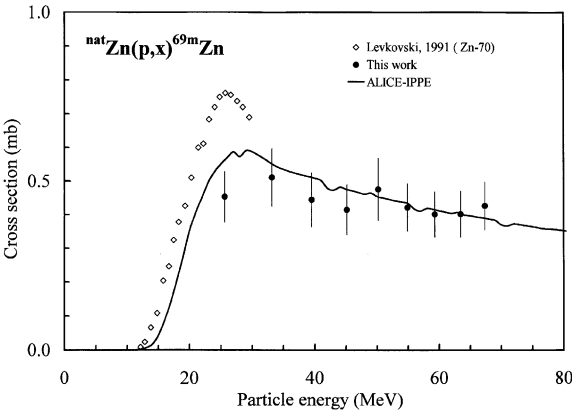

Fig. 5. Experimental and theoretical excitation function for production of ^{69m}Zn by proton irradiation of Zn.

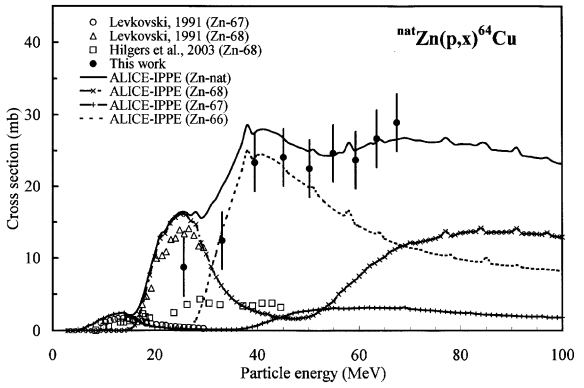

Fig. 6. Experimental and theoretical excitation function for production of ^{64}Cu by proton irradiation of Zn.

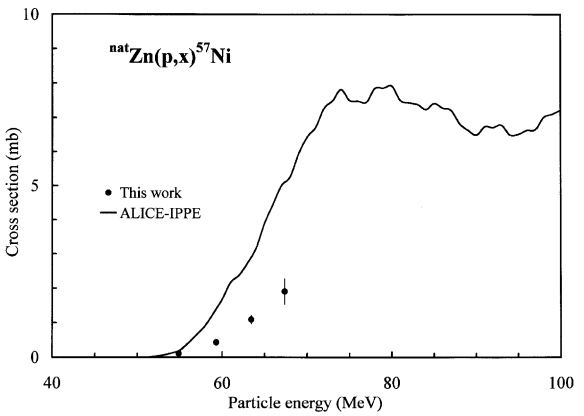

Fig. 7. Experimental and theoretical excitation function for production of ^{57}Ni by proton irradiation of Zn.

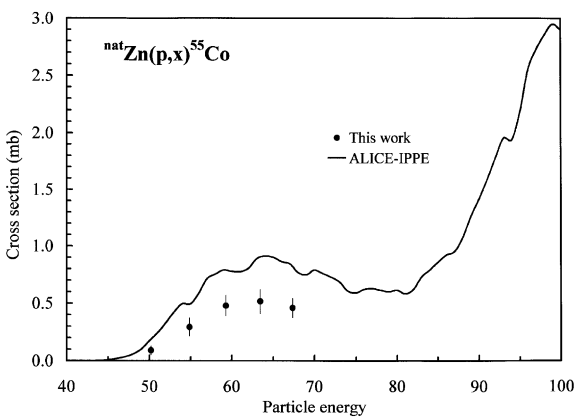

Fig. 8. Experimental and theoretical excitation function for production of ^{55}Co by proton irradiation of Zn.

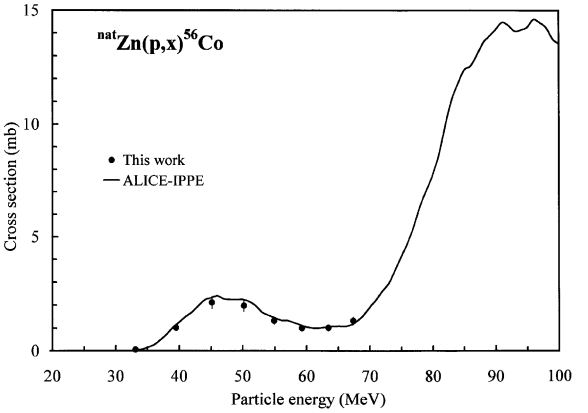

Fig. 9. Experimental and theoretical excitation function for production of ^{56}Co by proton irradiation of Zn.

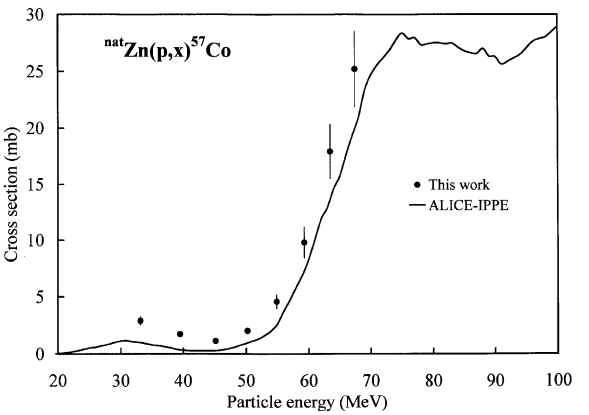

Fig. 10. Experimental and theoretical excitation function for production of ^{57}Co by proton irradiation of Zn.

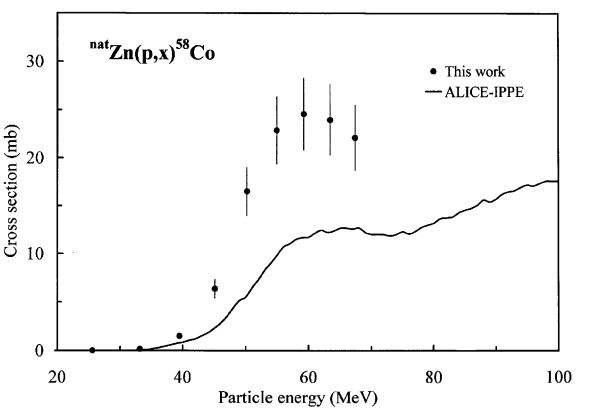

Fig. 11. Experimental and theoretical excitation function for production of ^{58}Co by proton irradiation of Zn.

contributing processes, to solve discrepancies in the earlier reported experimental data and to extrapolate below and beyond the investigated energy range possible.

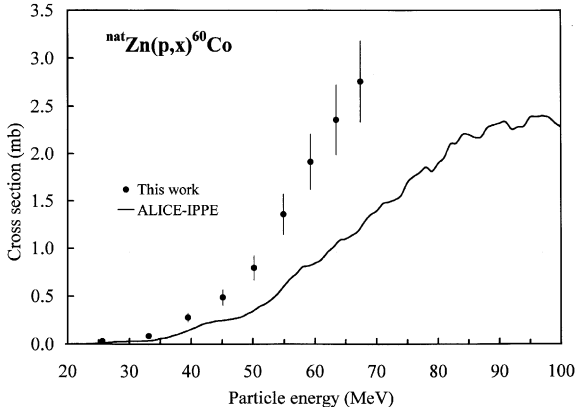

Fig. 12. Experimental and theoretical excitation function for production of ^{60}Co by proton irradiation of Zn.

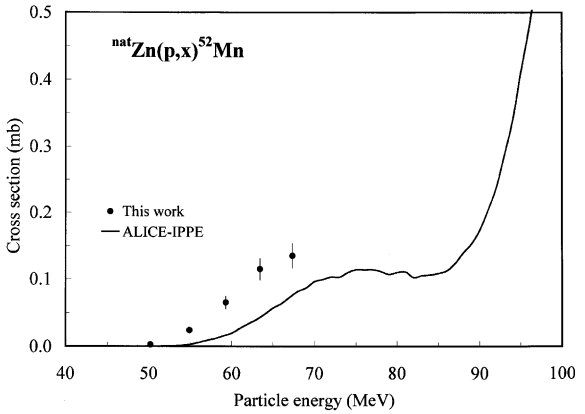

Fig. 13. Experimental and theoretical excitation function for production of ^{52}Mn by proton irradiation of Zn.

3.1. $^{nat}Zn(p,x)^{66}Ga$ process

^{66}Ga is a short-lived radioisotope used in nuclear medicine for PET imaging. It is produced directly in (p,x) reaction on ^{66,67,68,70}Zn isotopes. The highest yields are connected to the ^{66}Zn(p,n) and ^{68}Zn(p,3n) reactions. Several earlier experimental results are known for the production of ^{66}Ga on Zn target. In Fig. 1 cross-sections measured on Zn target of natural isotopic composition are collected including our new results. Cross-sections in low energy region were reported by a few authors (Bonardi and Birattari, 1983; Little and Lagunas-Solar, 1983; Kopecky, 1990; Hermanne, 1997; Hermanne et al., 1999). Data up to 200 MeV (Nortier et al., 1991) and recently up to 70 MeV (Szelecsényi et al., 2003) have been published. As it shown in Fig. 1 our data and the previous results agree well. The theoretical calculation overestimates the magnitude but describes well the shape of the excitation function.

3.2. $^{nat}Zn(p,x)^{67}Ga$ process

Production of ^{67}Ga was investigated in detail due to its importance in nuclear medicine as a diagnostic gamma emitter. Both the earlier reported data (Bonardi and Birattari, 1983; Little and Lagunas-Solar, 1983; Kopecky, 1990; Hermanne, 1997; Hermanne et al., 1999; Nortier et al., 1991) and the new experimental results measured on natural Zn are shown in Fig. 2. It should be noted that only a single data set was reported (Nortier et al., 1991) above 40 MeV.The agreement between our results and the previous experimental data as well as the theoretical calculation is fairly good. The observed two humps in the excitation function correspond to the ^{67}Zn(p,n) and ^{68}Zn(p,2n) reactions.

3.3. $^{nat}Zn(p,x)^{62}Zn$ process

The production of ^{62}Zn has importance as a generator for the positron emitting ^{62}Cu used for diagnostic study with PET. ^{62}Zn can be produced directly by (p,pxn)

Table 2
Measured cross-sections of the ^{nat}Zn(p,x)^{66,67}Ga,^{62,65,69m}Zn,^{64}Cu,^{57}Ni reactions

Energy (MeV)	σ (mb) ^{66}Ga	σ (mb) ^{67}Ga	σ (mb) ^{62}Ga	σ (mb) ^{65}Zn	σ (mb) ^{69m}Zn	σ (mb) ^{64}Cu	σ (mb) ^{57}Ni
67.4±0.3	15.0±2.3	11.2±1.7	26.4±3.4	99±13	0.43±0.07	28.9±6.3	1.90±0.37
63.4±0.5	15.1±2.5	11.6±1.8	25.4±3.2	106±14	0.40±0.07	26.7±6.2	1.09±0.13
59.3±0.6	16.8±2.7	12.9±2.0	25.7±3.3	110±15	0.40±0.07	23.7±5.4	0.437±0.054
54.9±0.8	18.4±2.9	13.3±2.1	26.9±3.4	122±17	0.42±0.07	24.6±5.7	0.111±0.022
50.2±1.0	23.7±3.8	14.0±2.2	33.0±4.2	124±18	0.48±0.09	22.5±5.6	
45.1±1.2	25.9±4.0	14.5±2.2	36.1±4.6	116±16	0.41±0.07	24.1±6.9	
39.5±1.4	42.6±7.6	16.8±2.6	43.4±5.6	103±14	0.44±0.08	23.3±7.4	
33.1±1.7	37.3±5.9	31.1±4.8	20.6±2.7	132±18	0.51±0.09	12.4±5.0	
25.6±2.0	24.4±3.6	109±12	1.65±0.33	211±29	0.45±0.08	8.7±3.6	

Table 3
Measured cross-sections of the $^{nat}Zn(p,x)^{55,56,57,58g,60}Co,^{52,54}Mn$ reactions

Energy (MeV)	σ (mb) ^{55}Co	σ (mb) ^{56}Co	σ (mb) ^{57}Co	σ (mb) ^{58}Co	σ (mb) ^{60}Co	σ (mb) ^{52}Mn	σ (mb) ^{54}Mn
67.4±0.3	0.46±0.08	1.32±0.17	25.2±3.3	22.1±3.4	2.76±0.42	0.13±0.02	1.07±0.12
63.4±0.5	0.52±0.10	1.01±0.14	17.9±2.4	24.0±3.7	2.36±0.37	0.11±0.02	0.49±0.06
59.3±0.6	0.48±0.09	1.00±0.13	9.81±1.36	24.6±3.8	1.91±0.29	0.065±0.010	0.17±0.02
54.9±0.8	0.29±0.08	1.32±0.17	4.57±0.61	22.9±3.5	1.36±0.21	0.024±0.005	0.056±0.012
50.2±1.0	0.090±0.038	1.97±0.25	2.03±0.27	16.5±2.5	0.79±0.13		
45.1±1.2		2.12±0.27	1.15±0.16	6.4±1.0	0.48±0.08		
39.5±1.4		1.01±0.13	1.74±0.23	1.51±0.23	0.28±0.05		
33.1±1.7		0.058±0.016	2.91±0.39	0.18±0.05	0.085±0.018		
25.6±2.0			1.37±0.17	0.019±0.011	0.032±0.010		

reactions and through its parent nuclei ^{62}Ga (116 ms) on the zinc target. We deduced the cumulative cross-section including contributions of both production routes. Only two earlier experimental data sets were found in the literature up to 35 MeV (Hermanne et al., 1999) and up to 70 MeV (Szelecsényi et al., 2003). Our new results, the earlier experimental data, and the theoretical calculations show good agreement (see Fig. 3). The maximal value of the excitation function corresponds to the reactions on ^{64}Zn having the highest isotopic abundance. A small energy shift is observed at the lowest energy point of our data series that can be explained probably with the large uncertainty of the bombarding energy at the end of the used stack.

3.4. $^{nat}Zn(p,x)^{65}Zn$ process

When bombarding the natural Zn target the ^{65}Zn radioisotope is produced directly and through the decay of ^{65}Ga ($T_{1/2}=15$ min). In this work we report cumulative cross-sections. Its production and decay characteristics make it very suitable for thin layer activation studies as a tracer. Only one earlier experimental data set was found in the literature (Bonardi and Birattari, 1983). The new experimental values and the results of the model calculations are shown in Fig. 4. The theory reproduces well the shapes of the excitation functions, but the absolute values are underestimated. The observed two humps correspond to reactions on ^{66}Zn and ^{68}Zn.

3.5. $^{nat}Zn(p,x)^{69m}Zn$ process

The ^{69}Zn radioisotope has two longer lived isomeric states. Due to the short half-life of the ground state (56 min) the directly produced ground state had decayed completely when we started our activity measurements. The applied long cooling time (more than one day) made possible to determine only the production cross-section of the longer lived ($T_{1/2}=13.8$ h) isomeric state, which decays mostly to the ground state. Only one process contributes to the production of ^{69m}Zn, the ^{70}Zn(p,pn) reaction. One earlier experimental data set was found on highly enriched ^{70}Zn target (Levkovski, 1991). For comparison we have the normalized data of Levkovski (1991) to natural composition. The experimental and theoretical data are shown in Fig. 5. For comparison we reproduced the result of the model calculations, which represents the sum of the cross-sections of the directly produced ground state and the cross-section of the isomeric state. The small overlapping energy region of our new data and the previous results (Levkovski, 1991) make it difficult to compare the two data sets. The only overlapping data point has large uncertainty due to the long stack used in our experiment. The model calculations can reproduce our results both in shape and magnitude. A good agreement can be explained with a very low population rate of the low spin ground state.

3.6. $^{nat}Zn(p,x)^{64}Cu$ process

The ^{64}Cu radioisotope is used in nuclear medicine both for radioimmuno-therapy and PET imaging. The activity of ^{64}Cu can be measured via the 511 keV annihilation line or the very weak (0.473%) 1345.8 keV gamma line following its β^+-decay. Considering the facts that we have used the natural Zn target and its activity is measured non-destructively, the number of ^{64}Cu atoms were determined via the 1345.8 keV gamma line. The low intensity of the gamma line due to the low branching ratio was enhanced by using 650 μm thick targets. Searching through the literature two related experimental works were found. Production cross-section data were reported on highly enriched ^{67}Zn and ^{68}Zn targets up to 29.5 MeV (Levkovski, 1991). Recently, the excitation function of the ^{68}Zn(p,αn)^{64}Cu reaction was investigated (Hilgers et al., 2003) by using highly enriched target material as well as chemical separation and the the 511 keV annihilation line was measured. In order to compare these two data sets with

our results, we normalized them to natural isotopic composition. Data are presented in Fig. 6. The results of ALICE-IPPE calculations for ^{nat}Zn target and for the independent contributions on ^{66,67,68}Zn-enriched zinc targets are also reproduced in Fig. 6 in order to explain the observed behaviour of the experimental data points. From the theoretical curves it can be deduced that the contribution of the reactions on ^{67}Zn is significant around 16 MeV and above 40 MeV due to the (p,α) and (p,2p2n) reactions, respectively. In general, at higher energies the (p,xpyn) process dominates. The reaction channels are open at ~25 MeV for the production of ^{64}Cu from ^{66}Zn having a maximum value around 40 MeV. The contribution of ^{68}Zn targets is important, around 25 MeV and above 60 MeV. The experimental data measured on enriched ^{68}Zn target by Levkovski (1991) are in good agreement with the theoretical results, but data measured by Hilgers et al. (2003) are much lower and their curve has an unusual shape. No explanation was found for this deviation. On the other hand, we have to mention that the data reported (Hilgers et al., 2003) on deuteron induced reactions were also found to be too low compared to other results. It indicates that it should be an explanation for the deviation independent of the investigated reactions. Taking into account that we used a well proved experimental technique, the systematic error of the measured data can be originated only from the error of the absolute intensity of the used 1346 keV gamma line of the ^{64}Cu. No background gamma line was found at the same energy from the decay of the simultaneously produced radioisotopes.

The agreement between our experimental data measured on natural Zn target and the result of the ALICE-IPPE model calculation is relatively good. We note that ^{64}Cu cannot be produced on ^{nat}Zn with a high radioisotope purity which has medical importance due to the simultaneously produced ^{67}Cu. The theoretical calculations help us to select the most productive route for ^{64}Cu by using highly enriched monoisotopic targets. Up to 30 MeV the ^{68}Zn(p,αn) reaction can be used, but the ^{66}Zn(p,x)^{64}Cu process is much more productive, with additional advantage of absence of ^{67}Cu (see Fig 6, the cross-sections of contributing reactions are normalized to isotopic abundance of natural Zn).

3.7. ^{nat}Zn(p,x) ^{57}Ni process

No earlier experimental data were found in the literature. We have measured experimental data at four energy points from 58 to 67 MeV (see Fig. 7). The theory overestimates the experimental data by a factor of two. According to the theoretical calculations, reactions produced on ^{64}Zn are the dominating process up to 100 MeV.

3.8. ^{nat}Zn(p,x)^{55}Co process

The measured excitation function and the result of the theoretical calculation are shown in Fig. 8. No earlier experimental results were found in the literature. The ^{64}Zn(p,2α2n) and ^{64}Zn(p,4p6n) reactions contribute to the resulting cross-section in the investigated energy range. The theory overestimates the measured cross-section. According to theoretical estimations, the production of ^{55}Ni is energetically not possible in the investigated energy range.

3.9. ^{nat}Zn(p,x)^{56}Co process

The measured cross-sections and the theoretical estimation are shown in Fig. 9. No earlier experimental data were found in the literature. In the measured spectra no activity of the ^{56}Ni ($T_{1/2}$ = 6.057 day) was found which is the possible parent nuclei of the ^{56}Co. The ^{56}Co is produced directly only in the investigated energy range. The observed maxima around 45 MeV is originating from the ^{64}Zn(p,2αn) reaction. A second maximum is predicted by the theory around 90 MeV from the ^{64}Zn(p,4p5n) process.

3.10. ^{nat}Zn(p,x)^{57}Co process

The activity of ^{57}Co was measured after the complete decay of the parent ^{57}Ni. The measured cross-sections are shown in Fig. 10. In the investigated energy range the theoretical calculations reproduce well the experimental values both in shape and absolute values. The two maxima around 30 and 75 MeV are originating from the ^{64}Zn(p,2α) and the ^{64}Zn(p,4p4n) reactions, respectively, on the most abundant ^{64}Zn. No experimental data were reported previously.

3.11. ^{nat}Zn(p,x)^{58}Co process

The cross-section of ^{nat}Zn(p,x)^{58}Co reaction (Fig. 11) was calculated by using gamma spectra measured after the complete decay of the ^{58m}Co isomeric state ($T_{1/2}$ = 8.94 h). ^{58}Ni is a stable isotope; therefore, the measured cumulative cross-section contains contribution only from the ^{58}Co. The theory significantly underestimates the experimental data. As in the case of the above discussed lighter Co radioisotopes, the reactions induced on ^{64}Zn give the largest contributing part to the measured cross-section in the investigated energy range. Above 70 MeV, the contribution of the reactions occurred on ^{66}Zn can also be seen.

3.12. ^{nat}Zn(p,x)^{60}Co process

The ground state ($T_{1/2}$ = 5.3 year) and the short-lived isomeric state ($T_{1/2}$ = 11 min) of ^{60}Co were produced

directly from Zn by neglecting the contribution through the decay of ^{60}Fe ($T_{1/2}=10^5$ year). Several reactions contribute to the complex process. Near the effective threshold of the excitation function the ^{67}Zn(p,2α) and ^{68}Zn(p,2αn) reactions give their contributions, but at higher energies the effects of (p,xpyn) reactions on ^{66,67,68}Zn become more dominant. The cross-section presented here for production of the ground state of ^{60}Co (see Fig. 12) is a cumulative process which contains the contribution from the internal decay of the short-lived isomeric state. No earlier experimental data were found in the literature. The theoretical values are lower by a factor of two as compared to the experimental data.

3.13. $^{nat}Zn(p,x)^{52}Mn$ process

The measured cross-sections are shown in Fig. 13, in comparison with the result of the ALICE-IPPE calculation. Up to 80 MeV the main contributing process is the ^{64}Zn(p,3αn) reaction. Above this energy the reactions on the same ^{64}Zn target with emission of separated single particles is becoming more significant and the (p,3α3n) reaction on ^{66}Zn is also becoming energetically possible.

3.14. $^{nat}Zn(p,x)^{54}Mn$ process

The results of our experiment and the model calculations are shown in Fig. 14. The theoretical curve is lower compared to the experimental values. The main contributing processes below 75 MeV are the ^{64}Zn(p,2α2pn) and the ^{66}Zn(p,3αn) reactions. Above this energy the ^{68}Zn(p,3α3n) reaction and the (p,xpxn) processes on ^{64}Zn and ^{66}Zn become energetically possible and start to dominate.

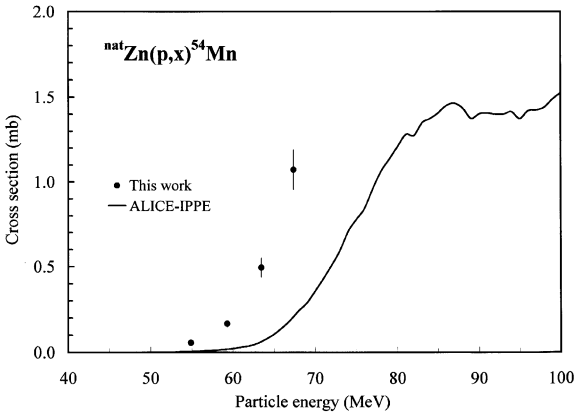

Fig. 14. Experimental and theoretical excitation function for production of ^{54}Mn by proton irradiation of Zn.

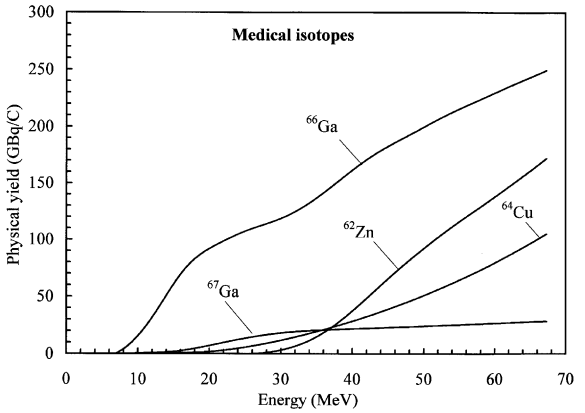

Fig. 15. Integral yields for production of medically related ^{66,67}Ga, ^{62}Zn and ^{64}Cu radioisotopes.

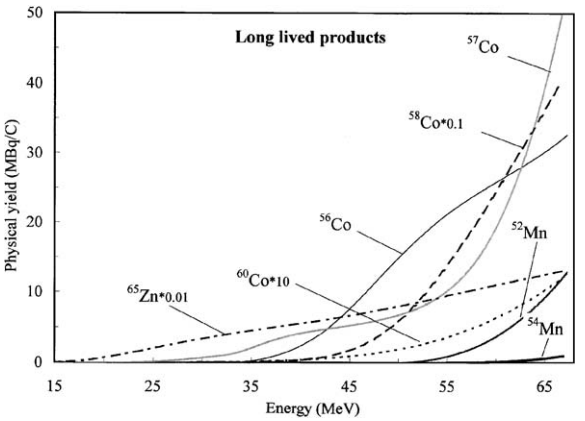

Fig. 16. Integral yields for production of long-lived ^{65}Zn, ^{56,57,58,60}Co and ^{52,54}Mn radioisotopes.

4. Integral yields

Integral yields as a function of the incident energy are closer to practical needs than the microscopic cross-sections. On the basis of the measured experimental data and the results of theoretical model calculations, the integral yields for the production of medically important radioisotopes ^{66,67}Ga, ^{62}Zn and ^{64}Cu on ^{nat}Zn were deduced. These data were also calculated for ^{65}Zn, ^{56,57,58,60}Co and ^{52,54}Mn long-lived reaction products. In order to estimate the yields up to 100 MeV, the theoretical curves were normalized to the experimental data in the overlapping energy region. The calculated yields are shown in Figs. 15 and 16. Experimental thick target yields were not reported in the literature except of a few data points for the medically related ^{66}Ga and ^{67}Ga isotopes at low energies.

5. Conclusions

New cross-section data were measured in the energy range 26–67 MeV for 13 reaction products, in most cases for the first time. Model calculations were carried out by using the Alice-IPPE code. The theoretical calculations describe well the shapes of the measured excitation functions in all cases. Integral yields were deduced for 11 processes and the practical applications of the reaction products that have been demonstrated. The experimental and theoretical data obtained in these investigations are useful in several applications like production of medically important radioisotopes by using ^{nat}Zn target, production of the ^{62}Zn(^{62}Cu) generator system, testing the cross-section data measured on highly enriched Zn targets (^{66}Ga, ^{67}Ga, ^{64}Cu), selecting and optimizing the most effective production routes (^{66}Zn(p,x)^{64}Cu 100–30 MeV), estimating impurity levels of the produced radioactive isotopes, and calculating dose and necessary shielding for radiation of waste (^{65}Zn, ^{56,57,58,60}Co and ^{52,54}Mn).

Acknowledgements

The authors are grateful to the operating staff of the cyclotron at the Tohoku University for performing the irradiations. This work was carried out in the frame of the scientific exchange program between the Japan Society for Promotion of Science (JSPS) and the Hungarian Academy of Sciences (HAS). This work was supported in part by the Hungarian Research Fund (OTKA T 037190). One of the authors (F. Ditrói) is a grantee of the Bolyai János Scholarship of the Hungarian Academy of Sciences.

References

Andersen, H.H., Ziegler, J.F., 1977. Hydrogen stopping powers and ranges in all elements. Handbook of Stopping Cross-Sections or Energetic Ions and Elements, vol. 3. Pergamon Press, New York.

Bonardi, M., Birattari, C., 1983. Optimization of irradiation parameters for ^{67}Ga production from ^{nat}Zn(p,xn) nuclear reactions. J. Radioanal. Chem. 76, 311.

Chu, S.Y.F., Ekstrom, L.P., Firestone, R.B., 1999. WWW Table of Radioactive Isotopes, database version, 1999-02-28 from URL, **http://nucleardata.nuclear.lu.se/nucleardata**.

Dityuk, A.I., Konobeyev, A.Yu., Lunev, V.P., Shubin, Yu.N., 1998. New version of the advanced computer code ALICE-IPPE, Report INDC (CCP)-410, IAEA, Vienna.

Guide to Expression of Uncertainty in Measurement. 1993. International Organisation for Standardization, Geneva (ISBN 92-67-10188-9).

Hermanne, A., 1997. Private communication, reported in Szelecsényi, et al. (1998). Appl. Radiat. Isot. 49, 1005.

Hermanne, A., Szelecsényi, F., Sonck, M., Takács, S., Tárkányi, F., Van den Winkel, P., 1999. New cross-section data on ^{68}Zn(p,2n)^{67}Ga and ^{nat}Zn(p,xn)^{67}Ga nuclear reactions for the development of a reference data base. J. Radioanal. Nucl. Chem. Art. 240, 623.

Hilgers, K., Stoll, T., Skakun, Y., Coenen, H.H., Qaim, S.M., 2003. Cross-section measurements of the nuclear reactions ^{nat}Zn(d,x)^{64}Cu, ^{66}Zn(d,α)^{64}Cu and ^{68}Zn(p,αn)^{64}Cu for production of ^{64}Cu and technical developments for small-scale production of ^{67}Cu via the ^{70}Zn(p,α)^{67}Cu process. Appl. Radiat. Isot. 59, 343.

Ido, T., Hermanne, A., Ditrói, F., Szűcs, Z., Mahunka, I., Tárkányi, F., 2002. Excitation functions of proton induced nuclear reactions on ^{nat}Rb from 30 to 70 MeV. Implication for the production of ^{82}Sr and other medically important Rb and Sr radioisotopes. Nucl. Instr. Meth. B. 194, 369.

Kopecky, P., 1990. Cross-sections and production yields of ^{66}Ga and ^{67}Ga for proton reactions in natural zinc. Appl. Radiat. Isot. 41, 606.

Levkovski, V.N., 1991. Cross-Section of medium Mass Nuclide Activation ($A=40$–100) by Medium Energy Protons and Alpha Particles. Inter-Vesi, Moscow.

Little, E., Lagunas-Solar, C., 1983. Cyclotron production of 67Ga. Cross-sections and thick-target yields for the ^{67}Zn(p,n) and ^{68}Zn(p,2n) reactions. Int. J. Appl. Radiat. Isot. 34, 631.

Nortier, F.M., Mills, S.J., Steyn, G.F., 1991. Excitation functions and yields of relevance to the production of ^{67}Ga by proton bombardment of ^{nat}Zn and ^{nat}Ge up to 100 MeV. Appl. Radiat. Isot. 42, 353.

Szelecsényi, F., Boothe, T.E., Takács, S., Tárkányi, F., Tavano, E., 1998. Evaluated cross-section and thick target yield data bases of Zn + p processes for practical applications. Appl. Radiat. Isot. 49, 1005.

Szelecsényi, F., Kovács, Z., van der Walt, T.N., Steyn, G.F., Suzuki, K., Okada, K., 2003. Investigation of the ^{nat}Zn(p,x)^{62}Zn nuclear process up to 70 MeV: a new ^{62}Zn/^{62}Cu generator. Appl. Radiat. Isot. 58, 377.

Tárkányi, F., Szelecsényi, F., Takács, S., 1991. Determination of effective bombarding energies and fluxes using improved stacked foil technique. Acta Radiologica. Suppl. 376, 72.

Tárkányi, F., Takács, S., Gul, K., Hermanne, A., Mustafa, M.G., Nortier, M., Oblozinsky, P., Qaim, S.M., Scholten, B., Shubin, Yu.N., Youxiang, Z., 2001. Beam monitor reactions in: Charged particle cross-section database for medical radioisotope production: diagnostic radioisotopes and monitor reactions. IAEA, Vienna, pp. 49–152, (Chapter 4). IAEA-TECDOC-1211, (**http://www.nds.or.at/medical**).